Monitoring ECE transformations of metal carbonyls by in situ spectroelectrochemistry; SNIFTIRS of $[Co_3(CO)_9C]_2$

Paula A. Brooksby, Noel W. Duffy, A. James McQuillan, Brian H. Robinson *, Jim Simpson

Department of Chemistry, University of Otago, PO Box 56 Dunedin, New Zealand

Abstract

An in situ subtractively normalised interfacial FTIR spectroscopy (SNIFTIRS) investigation of $[Co_3(CO)_9C]_2$ in dichloromethane is used to illustrate the application of these techniques to follow ECE transformations of metal carbonyls in a thin layer cell. SNIFTIRS data obtained at a platinum electrode show that the major species at ambient temperature is not the radical anion $[Co_3(CO)_9C]_2^{•-}$. Within the timescale of the measurement $[Co_3(CO)_9C]_2^{•-}$ transforms to a new species with a bridged carbonyl configuration; this species forms a chemically reversible redox couple in the thin layer. The consequences for the redox chemistry of $[Co_3(CO)_9C]_2$ are discussed. © 1999 Elsevier Science S.A. All rights reserved.

Keywords: Spectroelectrochemistry; Metal carbonyls; Cluster

1. Introduction

Many metal carbonyl clusters act as chemically reversible electrophores and electronic communication between linked cluster electrophores has been established [1,2]. If there is efficient energy transfer between electrophores they could be a component or precursor of new materials. For example, thermal release of CO from cobalt clusters produces solid material having metallic conduction as established by impedance spectroscopy [3]. Elucidation of the redox processes usually relies on standard electrochemical techniques but with metal carbonyl clusters strong adsorption on the electrode surface and short lifetimes of crucial intermediates often make it difficult to completely define the system. During the past two decades, in situ infrared spectroelectrochemical techniques have had increasing use for identifying species produced during electron transfer processes at electrodes [4]. Because $\nu(CO)$ bands are strong with energies in a window free from other absorptions, these in situ techniques are ideal for studying carbonyl cluster electrophores.

A convenient class of cluster electrophore to explore by in situ spectroelectrochemical techniques is the tricobaltcarbon clusters, $Co_3(CO)_9CR$, whose chemically reversible couples can be tuned by the judicious choice of R and ligand substitution [2,5]. An investigation of the infrared in situ spectroelectrochemistry of the $Co_3(CO)_9CPh$ cluster in methanol enabled the major reduction products of $Co_3(CO)_9CPh$ to be identified [6]. For the $Co_3(CO)_9CPh$ system the primary redox product $Co_3(CO)_9CPh^{•-}$ does not undergo any significant chemical transformations during an in situ thin layer investigation. Unfortunately, many reduced metal carbonyl clusters do not have this stability and they are prone to ECE reactions. One particularly interesting member of this class is the dimer $[Co_3(CO)_9C]_2$ in which there is a direct carbon–carbon link between the cluster redox units. The C–C bond distance from the crystal structure is 1.43 Å (both monoclinic [7] and trigonal [8] morphologies have been identified with slightly different C–C bond lengths). This relatively short bond indicates that electron density is transferred from the Co_3 electron-sink to the C–C link giving a capacity for intracluster electronic communication. Conventional electrochemistry in dichloromethane gave electrochemical responses at low temperatures compatible with two

---

* Corresponding author. Fax: + 64-3-4797906.
  E-mail address: chemmail@otago.ac.nz (B.H. Robinson)

consecutive one-electron transfers involving two electrochemically coupled redox centres [9]. The separation of 360 mV between the first and second reduction steps was similar to that for biferrocene [10], suggesting that there was very effective communication through the C–C bond. At ambient temperatures an additional ECE process was observed after the first electron transfer, but the role of this process in the succeeding electron transfer was not clear. The role of the ECE process may be more significant than first realised, as recent work has shown that $[Co_3(CO)_9C]_2$ will not participate in electron transfer catalysed substitution (ETC) reactions, a feature of other $Co_3(CO)_9CR$ clusters [2,11].

The $[Co_3(CO)_9C]_2$ system was therefore used to investigate, for the first time, whether in situ electrochemical techniques could assist in identifying short-lived intermediates from metal carbonyl redox reactions. We used an in situ methodology, subtractively normalised interfacial FTIR spectroscopy (SNIFTIRS) [4], which gives absorbance difference spectra induced by changes in electrode potential.

2. Results

All data reported herein were obtained in dichloromethane. Data from a SNIFTIRS experiment are not the instantaneous response that is observed in conventional voltammetry. SNIFTIR spectra are gathered at steady state conditions once the potential has been stepped to a new value. Hence a spectrum obtained at each potential is a time-averaged response (ca. 2 mins in our setup). The cyclic voltammetric results are, by comparison, the immediate response of the system to a perturbation. Ideal electrochemical cell behaviour is sacrificed in a SNIFTIRS thin-layer cell and large solution resistances often result. Hence, species produced during reduction and oxidation reactions may occur at potentials in the SNIFTIRS cell which are somewhat different from those in conventional electrochemical experiments. We have also observed that the condition and type of electrode surface influences the voltametric response.

Cyclic voltammograms of 1×10^{-3} mol dm^{-3} $[Co_3(CO)_9C]_2$ at 18°C taken as a reference for the SNIFTIRS experiment are shown in Fig. 1 (internal reference ferrocene). Fig. 1(A) is similar to that obtained with a standard electrochemical cell and the same labelling scheme has been used as in Ref. [9]. The main features **A**, **B**, **C**, seen on the initial scan between $+0.4$ and -1.4 V are all irreversible chemically at 18°C irrespective of whether the scans are switched after $\mathbf{A_c}$ or $\mathbf{B_c}$. Couple **C** is not seen on the first scan if the switching potential is before $\mathbf{A_c}$. A primary one-electron reduction at $\mathbf{A_c}$ to the radical anion
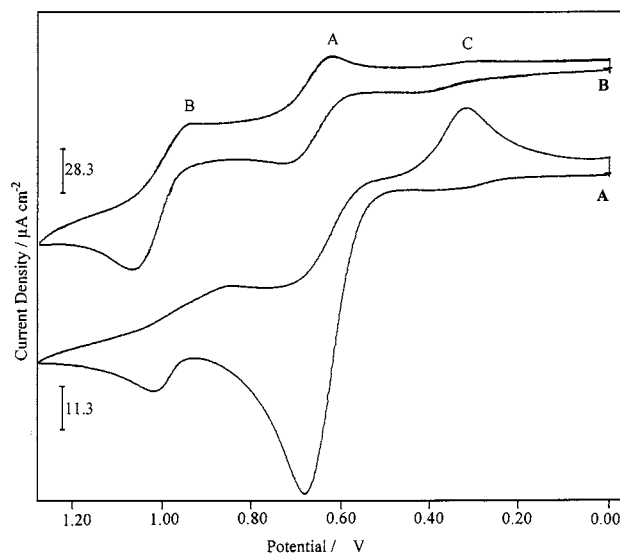

Fig. 1. (A) Cyclic voltammogram of 10^{-3} mol dm^{-3} $[Co_3(CO)_9C]_2$ in 0.1 mol dm^{-3} TBAP dichloromethane. Scan rate = 50 mV s^{-1}. Temperature 18°C. [ferrocene] = 10^{-3} mol dm^{-3}. Potential for $[Fc]^{+1/0}$ was 0.49 V. (B) Cyclic voltammogram of 10^{-3} mol dm^{-3} $[Co_3(CO)_9C]_2$ in 0.1 mol dm^{-3} TBAP dichloromethane. Scan rate = 50 mV s^{-1}. Temperature -40°C.

$[Co_3(CO)_9C]_2^{\bullet-}$ is followed by a rapid transformation to a new species which itself is oxidised back to $[Co_3(CO)_9C]_2$ at -0.33 V $[\mathbf{C_a}]$. At -40°C (Fig. 1(B)) (or at scan rates > 5 V s^{-1}) **B** approaches reversibility and although i_a/i_c is ca. 1 for couple **A** there is a remnant of a reversible couple **C**. Data obtained with solutions saturated with CO were the same as shown in Fig. 1. This indicates that the transformation of $[Co_3(CO)_9C]_2^{\bullet-}$ does not involve CO loss.

3. SNIFTIR spectra

In this technique species present at higher concentrations at the sampling potential (E_s) give rise to positive IR bands while those present at higher concentrations at the reference potential (E_b) give negative IR bands. The amount of material removed from the optical layer by diffusion is related to the time taken to complete the experiment, in this case 30 min, so the negative peaks do not necessarily disappear on reoxidation. Furthermore, permanent losses arise from the involvement of unstable species in irreversible systems. The spectrum of the bulk solvent and electrolyte do not change with potential and are not observed. In principle, it is possible to distinguish between adsorbed and solution species by recording spectra with both s-polarised and p-polarised light [4,12]. However, the complexity of ν(CO) profile for clusters makes it difficult to interpret the small changes which occur and only p-polarised spectra were obtained for $[Co_3(CO)_9C]_2$.

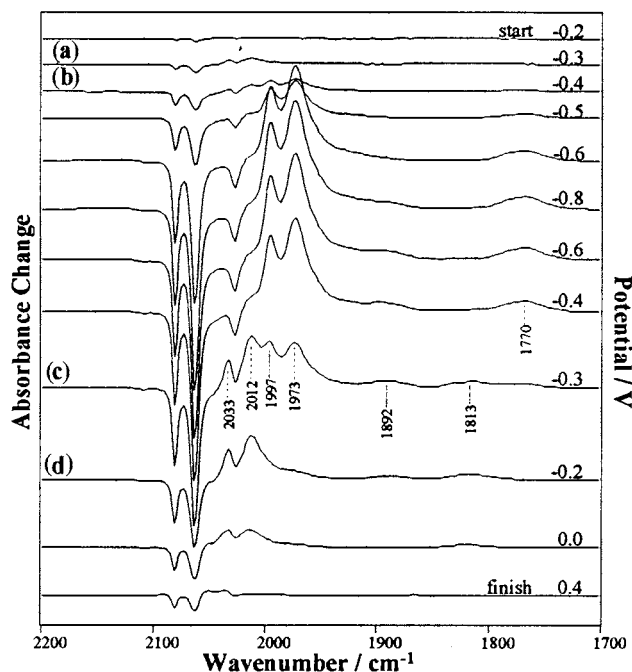Fig. 2. The SNIFTIR spectra for a solution of 5×10^{-4} mol dm^{-3} [Co$_3$(CO)$_9$C]$_2$ in 0.1 mol dm^{-3} TBAP dichloromethane. p-Polarised light. Negative steps starting from $E_b = 0.00$ V(SCE) followed by positive potential steps from -0.80 V.

Fig. 3. The SNIFTIR spectra for a solution of 5×10^{-4} mol dm^{-3} [Co$_3$(CO)$_9$C]$_2$ in 0.1 mol dm^{-3} TBAP dichloromethane. p-Polarised light. Negative steps starting from $E_b = 0.00$ V(SCE). Spectra labelled A–D are enhanced spectra of those shown in Fig. 3. $E_s =$ (A) -0.30 V (reduction scan); (B) -0.40 V (reduction scan); (C) -0.30 V (oxidation scan); (D) -0.20 V (oxidation scan).

Typical p-polarised SNIFTIR spectra for a solution of 5×10^{-4} mol dm^{-3} [Co$_3$(CO)$_9$C]$_2$ in 0.1 mol dm^{-3} TBAP/dichloromethane are shown in Fig. 2 with a negative potential limit at -0.80 V; that is, before couple **B**. Spectra marked with (a)–(d) in Fig. 2 are enlarged in Fig. 3. Spectra where the limit is extended out to -1.5 V to include **B** are shown in Fig. 4. In dichloromethane [Co$_3$(CO)$_9$C]$_2$ has ν(CO) bands at 2109(vw), 2081(s), 2064(vs), 2027(m) cm^{-1} but, realistically, only the last three bands will be obvious in SNIFTIR spectra. Two of these bands (2081, 2064 cm^{-1}) dominate the negative peaks in Figs. 2 and 3 increasing as [Co$_3$(CO)$_9$C]$_2$ is lost from the thin solution layer during reduction and then decreasing as it is regenerated on oxidation. A weak negative feature at 2027cm^{-1} accompanies this sequence and we assign this to the third observable ν(CO) band of [Co$_3$(CO)$_9$C]$_2$.

There are two major sets of *positive* (product) peaks in the voltage ramp $0.0 \rightarrow -0.80 \rightarrow 0.0$ V (Fig. 2) denoted as **Z** (2033, 2012, 1816 cm^{-1}) and **Z$^{\bullet-}$** (1997, 1973, 1770cm^{-1}). Corresponding sets were observed in the spectra of bulk electrochemically and chemically reduced solutions [9]. From 0.0 to -0.30 V (Fig. 3(A)) **Z** is the only species formed (the band at 2033 cm^{-1} is reduced in intensity because it overlaps with a band of the reactant). At -0.40 V both **Z** and **Z$^{\bullet-}$** are formed but **Z$^{\bullet-}$** dominates during the ramp $-0.40 \rightarrow -1.50 \rightarrow -0.40$ V. *The profiles of* Fig. 3(C,D) are mirror-images of Fig. 3(A,B).
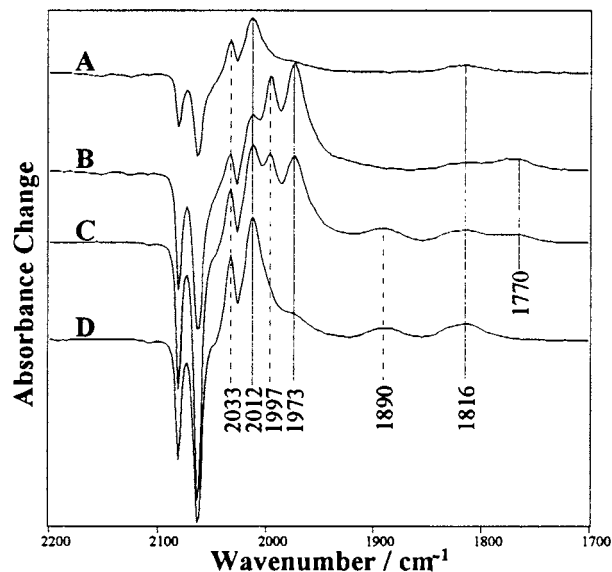
The unassigned band in Fig. 2 at 1890 cm^{-1} is due to Co(CO)$_4^-$ produced by decomposition of the radical anions and only present to any extent on the oxidation scan. This behavior is also observed during the
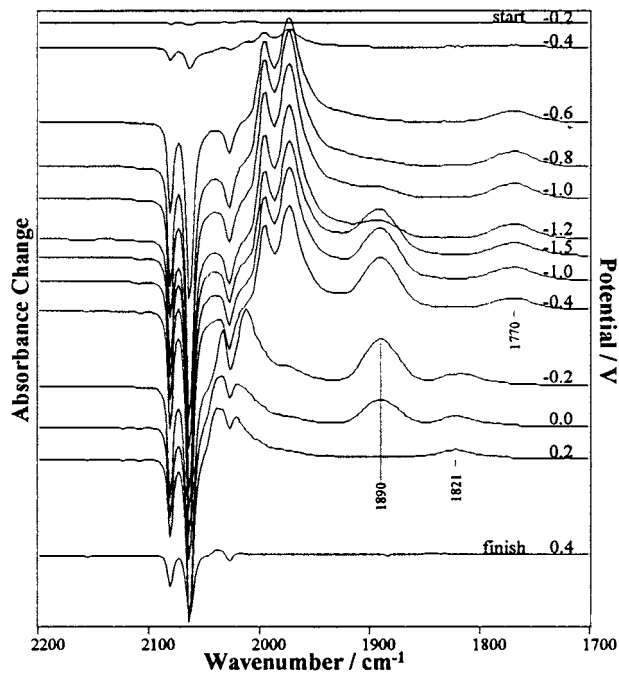

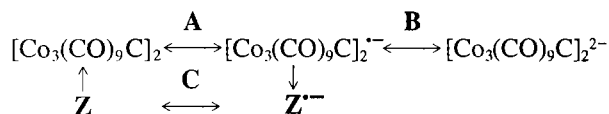Fig. 4. The SNIFTIR spectra for a solution of 5×10^{-4} mol dm^{-3} [Co$_3$(CO)$_9$C]$_2$ in 0.1 mol dm^{-3} TBAP dichloromethane. p-Polarised light. Negative steps starting from $E_b = 0.00$ V(SCE) followed by positive potential steps from -1.50 V.

SNIFTIRS for PhCCo$_3$(CO)$_9$ in methanol [6] and correlates with cyclic voltammetry. In the extended range (Fig. 4), $-0.20 \rightarrow -1.50 \rightarrow -0.20$ V, there is a new feature. A broad band **X** around 1900 cm^{-1} first appears at -1.20 V on the reduction scan, changes profile after -0.80 V on the oxidation scan and eventually resolves into the oxidation wave for Co(CO)$_4^-$.

4. Discussion

This SNIFTIRS investigation demonstrates that the technique is a valuable addition to the tools with which to probe ECE processes for metal carbonyl clusters. It is effectively a bulk electrolysis of material in the thin layer on a timescale which is compatible with that for chemical reactions. As such it gives a good picture of the species which may be involved in ETC reactions. SNIFTIRS data for [Co$_3$(CO)$_9$C]$_2$ agree in broad detail with those from standard OTTLE techniques [9] but from SNIFTIRS we have a clearer picture of the dominant species over chemically important time scales.

The ECE process follows the following cycle ([Co$_3$(CO)$_9$C]$_2$CO and [Co$_3$(CO)$_9$C]$_2$C$_2$ have equivalent ECE processes but the species related to **Z** are short-lived [9]):

$$[\text{Co}_3(\text{CO})_9\text{C}]_2 \underset{\text{C}}{\overset{\text{A}}{\longleftrightarrow}} [\text{Co}_3(\text{CO})_9\text{C}]_2^{\bullet-} \overset{\text{B}}{\longleftrightarrow} [\text{Co}_3(\text{CO})_9\text{C}]_2^{2-}$$

$$\mathbf{Z} \quad \overset{\text{C}}{\longleftrightarrow} \quad \mathbf{Z}^{\bullet-}$$

SNIFTIRS shows that **Z** and **Z**$^{\bullet-}$ comprise a chemically reversible redox system and because the [Co$_3$(CO)$_9$C]$_2^{\bullet-} \rightarrow$ **Z**$^{\bullet-}$ transformation is fast at ambient temperatures, **Z**$^{\bullet-}$ is the dominant species present in the thin layer in the potential range $-0.4 \leftrightarrow -0.80$ V. The v(CO) profile for **Z**$^{\bullet-}$ (and for **Z**) now includes a bridging v(CO) band. **Z** and **Z**$^{\bullet-}$ have the same CO configuration and cluster structure, which cannot be a gross modification of the parent since all data show that **Z** reverts rapidly to [Co$_3$(CO)$_9$C]$_2$. Furthermore, unlike classical voltammetry, the material is not being replenished in the thin layer so [Co$_3$(CO)$_9$C]$_2^{\bullet-}$ produced in the thin layer will reduce immediately any remaining **Z**.

The [Co$_3$(CO)$_9$C]$_2^{\bullet-}$ to **Z**$^{\bullet-}$ transformation is believed to involve an isomerisation of the CO-sphere to a bridged configuration. Since extraneous CO has no effect on the electrochemistry **Z** is unlikely to be coordinatively unsaturated. As the symmetry is effectively C_{3v} in either a non-bridged or bridged carbonyl configuration there is an a$_2^*$ LUMO in both structures [13]. Nevertheless, both the LUMO and HOMO will be perturbed by the electronic communication through the C–C bond. Electrode potentials are a function of the thermodynamic stability of both components of the

couple and it is not unreasonable that the [**Z**]$^{0/-}$ couple is *positive* of $\{[\text{Co}_3(\text{CO})_9\text{C}]_2\}^{0/-}$. The bridging carbonyl configuration should be a more efficient electron sink and the couple [Co$_3$(CO)$_8$CR]$^{0/-}$ is known to be positive of [Co$_3$(CO)$_9$CR]$^{0/-}$ [14]. The v(CO) bands of the two cluster units in the neutral [Co$_3$(CO)$_9$C]$_2$ are coupled strongly and it is difficult to predict what the effect of an extra electron in the delocalised LUMO will have on the energy of these bands. v(CO)[**Z**$^{\bullet-}$] bands are similar in energy to v(CO)[PhCCo$_3$(CO)$_9^{\bullet-}$] (1988 and 1977 cm^{-1}) representing a shift of ca. 70 cm^{-1} to lower energy from v(CO)[PhCCo$_3$(CO)$_9$] [6]. Unfortunately, the higher energy bands for **Z** may be obscured by the high intensity negative peaks at < -0.4 V and the apparently smaller shift of ca. 40 cm^{-1} from **Z** to **Z**$^{\bullet-}$ may be illusionary.

It is now possible to understand why [Co$_3$(CO)$_9$C]$_2$ is resistant to ETC substitution. The ETC mechanism requires both the primary radical anion and the substituted radical anion to have a finite lifetime [11]. Because of the [Co$_3$(CO)$_9$C]$_2^{\bullet-} \rightarrow$ **Z**$^{\bullet-}$ transformation the concentration of the primary species would be low. Furthermore, any [Co$_3$(CO)$_9$C]$_2^{\bullet-}$ produced in the cycle would be lost and hence the ETC cycle terminated. This implies that **Z**$^{\bullet-}$ is not activated for the substitution of a CO by a phosphine nor does it participate in efficient ETC cycles.

5. Experimental

The cluster [Co$_3$(CO)$_9$C]$_2$ was prepared as detailed in Ref. [9] and doubly crystallised from dichloromethane/hexane. All manipulations were carried out in an inert atmosphere. The dichloromethane was washed with a solution of water and sodium carbonate, dried over calcium chloride, fractionally distilled and collected over 4A molecular sieves. Tetrabutylammonium perchlorate (Fluka AG) was recrystallised from ethylacetate–pentane and dried at 80°C under vacuum.

5.1. Spectroscopy and electrochemistry

All potentials are with respect to an aqueous KCl saturated calomel electrode (SCE). *The potential of the ferrocene couple under these conditions was 0.49 V.* Electrode potential control, electrochemical data and SNIFTIR spectra were obtained using a EG&G Princeton Applied model 363 Potentiostat coupled to a HB Thompson & Associates model DRG16 Ramp Generator for cyclic voltammetry. Working potentials were monitored with a Thandar TM351 digital multimeter to an accuracy of 0.001 V. Cyclic voltammograms were recorded on a Houston X–Y recorder and digitally scanned and the SNIFTIR spectra on a Digilab 3200.

The Pt disc working electrodes used for the cyclic voltammograms and for the infrared spectroelectrochemical experiments were polished initially with 0.015 μm Al_2O_3 followed by electrochemical cleaning consisting of 30 s potential stepping between 4.0 and -4.0 V at 2 Hz in 0.5 mol dm^{-3} aqueous H_2SO_4 solution. This treatment gave well resolved adsorbed hydrogen peaks in a cyclic voltammogram recorded in 0.5 mol dm^{-3} H_2SO_4 aqueous solution. The electrode was then rinsed successively with water, dichloromethane and a portion of the cell solution before being placed in the spectroelectrochemical cell without allowing the electrode surface to dry at any stage of the rinsing. A conventional electrochemical cell with a 2.5 mm diameter polycrystalline platinum disc electrode was used to record the cyclic voltammograms at different temperatures. The SNIFTIRS experiments were performed at ambient temperatures. FTIR spectra were obtained with a Digilab FTS60V evacuable optical bench spectrometer equipped with an MCT detector and coupled to a thin-layer electrochemical cell via a CaF_2 prism. All spectra were recorded at 4 cm^{-1} resolution with an acquisition time of 60 s at each potential after 30 s was allowed for steady state conditions to be achieved. The noise level over most of the spectral range was about 2×10^{-4} absorbance. The IR reflectance accessory and SNIFTIRS cell (Chemistry Department, University of Otago) were designed to fit into the sample compartment of the Digilab bench [12]. The main body of the SNIFTIRS cell was housed externally to the bench. The cell body was constructed from Kel-F (Fluorocarbon, CA, USA). The cell included facilities for gas purging, a reference electrode (RE) compartment separated from the Pt working electrode (WE) by a Luggin capillary and a Pt wire (1 mm diameter) secondary electrode (SE) encircling the WE about 3 mm from the front of the cell. The platinum WE was a 9 mm diameter circular disc attached to a brass rod and encased in a cylindrical Kel-F rod so that only the front electrode surface was in contact with solution. The spectra were obtained with a solution layer of about 5 μm between the electrode and the CaF_2 prism. The WE assembly was machine finished to fit into the SNIFTIRS cell body in the vertical position. The IR beam was diverted from its normal path through the sample chamber onto the electrode surface by a reflectance accessory.

References

[1] N.G. Connelly, W. Geiger, Adv. Organometal. Chem. 24 (1985) 87.

[2] B.H. Robinson, J. Simpson, in: M. Chanon (Ed.), Paramagnetic Organometallic Species in Activation/Selectivity Catalysis, Kluwer, Dordrecht, 1989, p. 357.

[3] G.H. Worth, B.H. Robinson, J. Simpson, App. Organometal. Chem. 4 (1990) 481.

[4] R.J. Gale (Ed.), Spectroelectrochemistry: Theory and Practice, Plenum Press, NY, 1988

[5] B.M. Peake, B.H. Robinson, J. Simpson, D.J. Watson, Inorg. Chem. 16 (1977) 410. A.M. Bond, P.A. Dawson, B.M. Peake, P.H. Rieger, B.H. Robinson, J. Simpson, Inorg. Chem. 18 (1979) 1413. A.J. Downard, B.H. Robinson, J. Simpson, Organometallics 5 (1986) 1132.

[6] P.A. Brooksby, N.W. Duffy, A.J McQuillan, B.H. Robinson, J. Simpson, J. Chem Soc. Dalton Trans. (1998) 2855

[7] B.R. Penfold, M.D. Brice, Inorg. Chem. 11 (1972) 1381.

[8] U. Geiser, A.M. Kini, Acta Cryst. C49 (1993) 1322.

[9] B.H. Robinson, J. Simpson, G.H. Worth, Organometallics 11 (1992) 501. B.H. Robinson, J. Simpson, G.H. Worth, Organometallics 11 (1992) 3863.

[10] W.H. Morrison, S. Krogsrud, D.N. Hendrickson, Inorg. Chem. 12 (1973) 1998.

[11] C.M. Arewgoda, B.H. Robinson, J. Simpson, J. Chem. Soc. Chem. Commun. (1982) 284. G.J. Bezems, P.H. Rieger, S.J. Visco, J. Chem. Soc. Chem. Commun. (1981) 265. C.M. Arewgoda, B.H. Robinson, J. Simpson, J. Am. Chem. Soc. 105 (1983) 1893. A.J. Downard, B.H. Robinson, J. Simpson, Organometallics 5 (1986) 1140.

[12] J.G. Love, A.J. McQuillan, J. Electroanal. Chem. 274 (1989) 263. A. Babaei, A.J. McQuillan, J. Phys. Chem. 101 (1997) 7443.

[13] B.E.R. Schilling, R. Hoffmann, J. Am. Chem. Soc. 101 (1979) 3456.

[14] K. Hinkelmann, J. Heinze, H.-T. Schacht, J.S. Field, H. Vahrenkamp, J. Am. Chem. Soc. 111 (1989) 5078.